SIAM J. APPL. MATH.
Vol. 68, No. 5, pp. 1223–1246

DIFFUSION OF PROTEIN RECEPTORS ON A CYLINDRICAL DENDRITIC MEMBRANE WITH PARTIALLY ABSORBING TRAPS*

PAUL C. BRESSLOFF†, BERTON A. EARNSHAW†, AND MICHAEL J. WARD‡

Abstract. We present a model of protein receptor trafficking within the membrane of a cylindrical dendrite containing small protrusions called spines. Spines are the locus of most excitatory synapses in the central nervous system and act as localized traps for receptors diffusing within the dendritic membrane. We treat the transverse intersection of a spine and dendrite as a spatially extended, partially absorbing boundary and use singular perturbation theory to analyze the steady-state distribution of receptors. We compare the singular perturbation solutions with numerical solutions of the full model and with solutions of a reduced one-dimensional model and find good agreement between them all. We also derive a system of Fokker–Planck equations from our model and use it to exactly solve a mean first passage time (MFPT) problem for a single receptor traveling a fixed axial distance along the dendrite. This is then used to calculate an effective diffusion coefficient for receptors when spines are uniformly distributed along the length of the cable and to show how a nonuniform distribution of spines gives rise to anomalous subdiffusion.

Key words. protein receptor trafficking, diffusion-trapping, matched asymptotics, singular perturbation theory

AMS subject classification. 92C20

DOI. 10.1137/070698373

1. Introduction.

Neurons are amongst the largest and most complex cells in biology. Their intricate geometry presents many challenges for cell function, in particular with regard to the efficient delivery of newly synthesized proteins from the cell body or soma to distant locations on the axon or dendrites. The axon contains ion channels for action potential propagation and presynaptic active zones for neurotransmitter release, whereas each dendrite contains postsynaptic domains (or densities) where receptors that bind neurotransmitter tend to cluster. At most excitatory synapses in the brain, the postsynaptic density is located within a dendritic spine, which is a small, submicrometer membranous extrusion that protrudes from a dendrite. Typically spines have a bulbous head which is connected to the parent dendrite through a thin spine neck. Given that hundreds or thousands of synapses and their associated spines are distributed along the entire length of a dendrite, it follows that neurons must traffic receptors and other postsynaptic proteins over long distances (several 100μm) from the soma. This can occur by two distinct mechanisms: either by lateral diffusion in the plasma membrane [8, 26, 1, 7] or by motor-driven intracellular transport along microtubules followed by local insertion into the surface membrane (exocytosis) [17, 20, 29]. It is likely that both forms of transport occur in dendrites, depending on the type of receptor and the developmental stage of the organism.

*Received by the editors July 25, 2007; accepted for publication (in revised form) December 26, 2007; published electronically April 2, 2008. This work was supported by the NSF (DMS 0515725 and RTG 0354259).

http://www.siam.org/journals/siap/68-5/69837.html

†Department of Mathematics, University of Utah, 155 S. 1400 E., Salt Lake City, UT 84112 (bressloff@math.utah.edu, earnshaw@math.utah.edu).

‡Department of Mathematics, University of British Columbia, Vancouver, BC, V6T1Z2, Canada (ward@math.ubc.ca).

Recently, we constructed a one-dimensional diffusion-trapping model for the surface transport of AMPA (α-amino-3-hydroxy-5-methyl-4-isoxazole-propionic acid) receptors along a dendrite [6]. AMPA receptors respond to the neurotransmitter glutamate and mediate the majority of fast excitatory synaptic transmission in the central nervous system. Moreover, there is a large body of experimental evidence suggesting that the fast trafficking of AMPA receptors into and out of spines contributes to activity-dependent, long-lasting changes in synaptic strength [21, 22, 4, 8, 9, 16]. Single-particle tracking experiments suggest that surface AMPA receptors diffuse freely within the dendritic membrane until they encounter a spine [13, 26]. If a receptor flows into a spine, then it is temporarily confined by the geometry of the spine and through interactions with scaffolding proteins and cytoskeletal elements [4, 8]. A surface receptor may also be internalized via endocytosis and stored within an intracellular pool, where it is either recycled to the surface via exocytosis or degraded [11]. Motivated by these experimental observations, we modeled the surface transport of receptors along a dendrite as a process of diffusion in the presence of spatially localized, partially absorbing traps [6]. One of the major simplifications of our model was to reduce the cylindrical like surface of a dendrite to a one-dimensional domain by neglecting variations in receptor concentration around the circumference of the cable relative to those along the cable. We also neglected the spatial extent of each spine by treating it as a homogeneous compartment that acts as a point-like source/sink for receptors on the dendrite. This was motivated by the observation that the spine neck, which forms the junction between a synapse and its parent dendrite, varies in radius from 0.02–0.2μm [23]. This is typically an order of magnitude smaller than the spacing between neighboring spines and the radius of the dendritic cable (around 1μm). In the one-dimensional case, the introduction of point-like spines does not lead to any singularities since the associated one-dimensional Green's function for diffusion is a pointwise bounded function. We were thus able to calculate explicitly the steady-state distribution of receptors along the dendrite and spines, as well as to determine the mean first passage time (MFPT) for a receptor to reach a certain distance from the soma. This allowed us to investigate the efficacy of diffusive transport as a function of various biophysical parameters such as surface diffusivity and the rates of exo/endocytosis within each spine.

In this paper we extend our diffusion-trapping model to the more realistic case of a two-dimensional cylindrical surface. However, since the two-dimensional Green's function has logarithmic singularities, we can no longer neglect the spatial extent of a spine. Therefore, we proceed by solving the steady-state diffusion equation on a finite cylindrical surface containing a set of small, partially absorbing holes, which represent the transverse intersections of the spines with the dendrite. The solution is constructed by matching appropriate "inner" and "outer" asymptotic expansions [27, 25, 28, 24]. This leads to a system of linear equations that determines the dendritic receptor concentration on the boundary between the dendrite and each spine. We numerically solve these equations and use this to construct the steady-state distribution of receptors along the dendrite. We compare our results with numerical solutions of the full model and with a reduced one-dimensional model.

A brief outline of this paper is as follows: In section 2 we formulate our diffusion-trapping model for receptor trafficking on the boundary of a cylindrical dendritic cable. In section 3 we construct the steady-state solution to this model using singular perturbation techniques in the limit of small spine radii. In section 4 we present some numerical experiments for realistic physiological parameter values that compare our asymptotic solution of section 3 with both full numerical solutions and with the

solution of a one-dimensional approximation valid for a large aspect ratio dendritic cable. Finally, in section 5 we asymptotically calculate the MFPT for the diffusion of a single tagged receptor.

2. Diffusion-trapping model on a cylinder. Consider a population of N dendritic spines distributed along a cylindrical dendritic cable of length L and radius l as shown in Figure 2.1(A). Since protein receptors are much smaller than the length and circumference of the cylinder, we can neglect the extrinsic curvature of the membrane. Therefore, as shown in Figure 2.1(B), we represent the cylindrical surface of the dendrite as a long rectangular domain Ω_0 of width $2\pi l$ and length L so that

$$\Omega_0 \equiv \{(x,y) : 0 < x < L\,, |y| < \pi l\}.$$

The cylindrical topology is preserved by imposing periodic boundary conditions along the circumference of the cylinder, that is, at $y = \pm\pi l$. At one end of the cylinder ($x = 0$) we impose a nonzero flux boundary condition, which represents a constant source of newly synthesized receptors from the soma, and at the other end ($x = L$) we impose a no-flux boundary condition. Each spine neck is assumed to intersect the dendritic surface transversely such that the intersection is a circle of radius $\varepsilon\rho$ centered about the point $\mathbf{r}_j = (x_j, y_j) \in \Omega_0$, where $j = 1, \ldots, N$ labels the jth spine. For simplicity, we take all spines to have the same radius. Since a dendrite is usually several hundred μm in length, we will assume the separation of length scales $\varepsilon\rho \ll 2\pi l \ll L$. We then fix the units of length by setting $\rho = 1$ such that $2\pi l = \mathcal{O}(1)$ and treat ε as a small dimensionless parameter. Finally, we denote the surface of the cylinder excluding the small discs arising from the spines by Ω_ε so that

$$\Omega_\varepsilon = \Omega_0 \setminus \bigcup_{j=1}^{N} \Omega_j, \quad \Omega_j = \{\mathbf{r} : |\mathbf{r} - \mathbf{r}_j| \le \varepsilon\}.$$

Let $U(\mathbf{r}, t)$ denote the concentration of surface receptors within the dendritic membrane at position $\mathbf{r} \in \Omega_\varepsilon$ at time $t \in \mathbf{R}_+$. As a result of the small area of each spine, we assume that the receptor concentrations within each spine are spatially homogeneous. We let $R_j(t)$ denote the concentration of surface receptors in the jth spine. The dendritic surface receptor concentration evolves according to the diffusion equation

$$\frac{\partial U}{\partial t} = D\nabla^2 U, \quad (\mathbf{r}, t) \in \Omega_\varepsilon \times \mathbf{R}_+ \tag{2.1}$$

for a homogeneous surface diffusivity D, with periodic boundary conditions at the ends $y = \pm\pi l$,

$$U(x, \pi l, t) = U(x, -\pi l, t), \quad \partial_y U(x, \pi l, t) = \partial_y U(x, -\pi l, t), \tag{2.2}$$

and nonzero or zero flux conditions at the ends $x = 0, L$,

$$\partial_x U(0, y, t) = -\sigma \equiv -\frac{\sigma_0}{2\pi l D}\,, \quad \partial_x U(L, y, t) = 0. \tag{2.3}$$

Here σ_0 denotes the number of receptors per unit time entering the surface of the cylinder from the soma. At each interior boundary $\partial\Omega_j$ we impose the mixed boundary condition

$$\varepsilon\partial_n U(\mathbf{r}, t) = -\frac{\omega_j}{2\pi D}(U(\mathbf{r}, t) - R_j), \quad \mathbf{r} \in \partial\Omega_j, \quad j = 1, \ldots, N, \tag{2.4}$$

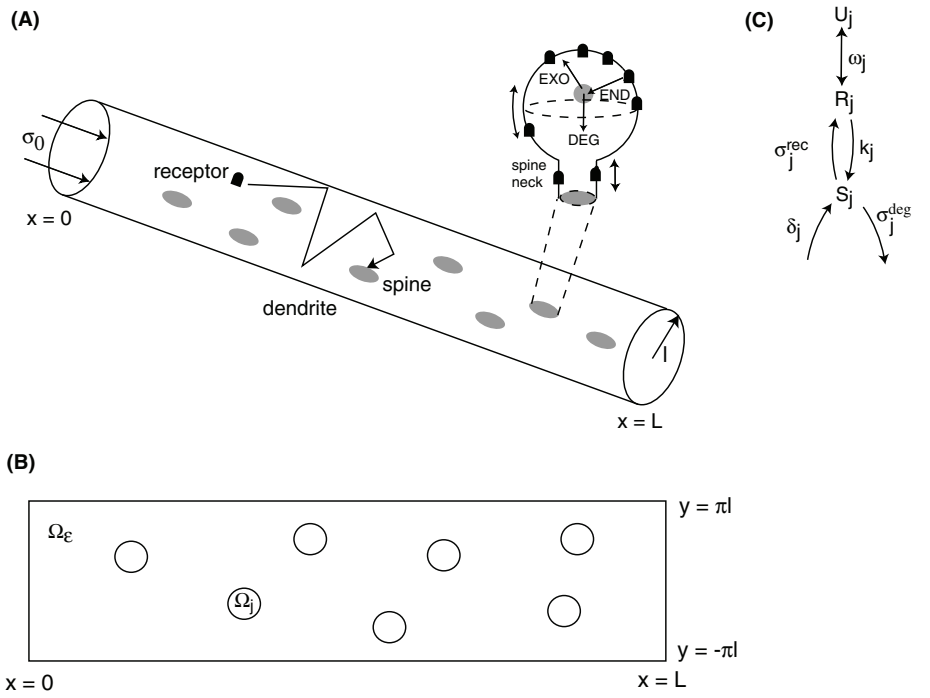

FIG. 2.1. *Diffusion-trapping model of receptor trafficking on a cylindrical dendritic cable (diagram not to scale).* (A) *A population of dendritic spines is distributed on the surface of a cylinder of length L and radius l. Each receptor diffuses freely until it encounters a spine where it may become trapped. Within a spine receptors may be internalized via endocytosis (END) and then either recycled to the surface via exocytosis (EXO) or degraded (DEG); see the inset. Synthesis of new receptors at the soma and insertion into the plasma membrane generates a surface flux σ_0 at one end of the cable.* (B) *Topologically equivalent rectangular domain with opposite sides $y = \pm\pi l$ identified.* (C) *State transition diagram for a simplified one-compartment model of a dendritic spine. Here R_j denotes the concentration of surface receptors inside the jth spine, U_j is the mean dendritic receptor concentration on the boundary between the spine neck and dendrite, and S_j is the number of receptors within the corresponding intracellular pool. Freely diffusing surface receptors can enter/exit the spine at a hopping rate ω_j, be endocytosed at a rate k_j, be exocytosed at a rate σ_j^{rec}, and be degraded at a rate σ_j^{deg}. New intracellular receptors are produced at a rate δ_j.*

where $\partial_n U$ is the outward normal derivative to Ω_ε. The flux of receptors across the boundary between the dendrite and jth spine is taken to depend on the difference in concentrations on either side of the boundary with ω_j an effective hopping rate. (This rate is determined by the detailed geometry of the spine [2].) It follows that the total number of receptors crossing the boundary per unit time is $\omega_j[U_j(t) - R_j(t)]$, where $U_j(t)$ is the mean dendritic receptor concentration on the boundary $\partial\Omega_j$ of the jth spine of length $2\pi\varepsilon$:

$$U_j = \frac{1}{2\pi\varepsilon}\int_{\partial\Omega_j} U(\mathbf{r},t)\,d\mathbf{r}. \tag{2.5}$$

Surface receptors within the jth spine can be endocytosed at a rate k_j and stored in an intracellular pool. Intracellular receptors are either reinserted into the surface via exocytosis at a rate σ_j^{rec} or degraded at a rate σ_j^{deg}. We also allow for a local source of intracellular receptors with a production rate δ_j. Denoting the number of

receptors in the jth intracellular pool by $S_j(t)$, we then have the pair of equations

$$\frac{dR_j}{dt} = \frac{\omega_j}{A_j}[U_j - R_j] - \frac{k_j}{A_j}R_j + \frac{\sigma_j^{rec}S_j}{A_j}\,, \tag{2.6}$$

$$\frac{dS_j}{dt} = -\sigma_j^{rec}S_j - \sigma_j^{deg}S_j + k_jR_j + \delta_j. \tag{2.7}$$

The first term on the right-hand side of (2.6) represents the exchange of surface receptors between the spine and parent dendrite. Since $\omega_j[U_j - R_j]$ is the number of receptors per unit time flowing across the junction between the dendritic cable and the spine, it is necessary to divide through by the surface area A_j of the spine in order to properly conserve receptor numbers. Note that in our previous one-dimensional model [6] we absorbed the factor of A_j into our definition of the rate of endocytosis k_j. (The precise variation of endocytic rate with spine area A_j will depend upon whether or not endocytosis is localized to certain hotspots within the spine [4].) The various processes described by (2.6) and (2.7) are summarized in Figure 2.1(C).

3. Steady-state analysis using asymptotic matching. In steady-state one can solve (2.6) and (2.7) for R_j in terms of the mean concentration U_j to get

$$R_j = \frac{\omega_jU_j}{\omega_j + k_j(1-\lambda_j)} + \frac{\lambda_j\delta_j}{\omega_j + k_j(1-\lambda_j)}, \tag{3.1}$$

where

$$\lambda_j \equiv \frac{\sigma_j^{rec}}{\sigma_j^{rec} + \sigma_j^{deg}}, \quad S_j = \frac{\lambda_j}{\sigma_j^{rec}}\left(k_jR_j + \delta_j\right). \tag{3.2}$$

Then U_j is determined from (2.5) and the steady-state version of (2.1):

$$\nabla^2 U = 0\,, \quad \mathbf{r} \in \Omega_\varepsilon, \tag{3.3}$$

with boundary conditions

$$U(x,\pi l) = U(x,-\pi l)\,, \quad \partial_y U(x,\pi l) = \partial_y U(x,-\pi l), \tag{3.4}$$

$$\partial_x U(0,y) = -\sigma, \quad \partial_x U(L,y) = 0, \tag{3.5}$$

where $\sigma = \sigma_0/(2\pi lD)$ from (2.3) and

$$\varepsilon\partial_n U(\mathbf{r}) = -\frac{\omega_j}{2\pi D}(U(\mathbf{r}) - R_j), \quad \mathbf{r} \in \partial\Omega_j\,, \quad j = 1,\ldots,N. \tag{3.6}$$

Since the radius of each spine is asymptotically small, we can make the simplification that $U(\mathbf{r}) = U_j$ on $\partial\Omega_j$. The substitution of (3.1) into (3.6) then yields the following reduced condition on the boundary of each spine:

$$\varepsilon\partial_n U(\mathbf{r}) = -\frac{\widehat{\omega}_j}{2\pi D}(U_j - \widehat{R}_j)\,, \quad \mathbf{r} \in \partial\Omega_j\,, \quad j = 1,\ldots,N, \tag{3.7}$$

where $\widehat{\omega}_j$ and $\widehat{R}_j$ are defined by

$$\widehat{\omega}_j \equiv \frac{\omega_j k_j(1-\lambda_j)}{\omega_j + k_j(1-\lambda_j)}\,, \qquad \widehat{R}_j \equiv \frac{\sigma_j^{rec}}{k_j}\frac{\delta_j}{\sigma_j^{deg}}. \tag{3.8}$$

Under steady-state conditions, one can view $\widehat{\omega}_j$ as an effective spine-neck hopping rate and $\widehat{R}_j$ as an effective receptor concentration within the spine.

Upon integrating the diffusion equation (3.3) over the domain Ω_ε and imposing the boundary conditions (3.4), (3.5), and (3.7), we obtain the solvability condition

$$\sigma_0 = \sum_{j=1}^{N} \widehat{\omega}_j \left[U_j - \widehat{R}_j\right]. \tag{3.9}$$

This expresses the condition that the rate at which receptors enter the dendrite from the soma is equal to the effective rate at which receptors exit the dendrite into spines and are degraded. Note that in the limit of negligible degradation of receptors in the intracellular pools so that $\sigma_j^{deg} \to 0$, it follows from (3.2) and (3.8) that $\lambda_j \to 1$, $\widehat{\omega}_j \to 0$, $\widehat{R}_j \to \infty$ with $\widehat{\omega}_j \widehat{R}_j \to -\delta_j$. Consequently, in the limit $\sigma_j^{deg} \to 0$, (3.9) reduces to $\sigma_0 \to -\sum_{j=1} \delta_j$, which has no solution for $\sigma_0 > 0$ and positive production rates $\delta_j > 0$. This shows that there is no steady-state solution when $\sigma_j^{deg} = 0$, as the number of receptors in the dendrite would grow without bound as time increases. A similar argument shows that there is also no steady-state solution in the limit of infinite spine-neck resistances such that $\omega_j \to 0$ for $j = 1, \ldots, N$. In this limit, newly synthesized receptors at the soma would not be able to diffuse from the dendrite to a spine and be degraded.

Our method of solution for the boundary value problem given by (3.3), (3.4), (3.5), and (3.7), which we denote by BVPI, proceeds in two steps. First, we solve a related problem, denoted by BVPII, in which the mixed boundary conditions (3.7) are replaced by the inhomogeneous Dirichlet conditions

$$U(\mathbf{r}) = U_j\,, \quad \mathbf{r} \in \partial\Omega_j, \quad j = 1, \ldots, N, \tag{3.10}$$

under the assumption that the U_j are known. In the singularly perturbed limit $\varepsilon \to 0$, the approximate solution for U valid away from each of the spines is shown below to be determined up to an arbitrary constant χ. Then, by substituting our asymptotic solution to BVPII into the N mixed boundary conditions (3.7) and upon satisfying the conservation equation (3.9), we obtain $N + 1$ linear equations for the $N + 1$ unknowns χ and $U_j, j = 1, \ldots, N$. This closed linear system of equations can be solved numerically to generate the full solution to the original boundary value problem BVPI. In order to solve BVPII asymptotically in the limit of small spine radii $\varepsilon \to 0$, we match appropriate "inner" and "outer" asymptotic expansions, following along similar lines to previous studies of boundary value problems in domains with small holes [27, 25, 28, 24].

3.1. Matching inner and outer solutions. Around each small circle $\partial\Omega_j$ we expect the solution of BVPII to develop a boundary layer where it changes rapidly from its value U_j on $\partial\Omega_j$ to another value that is required by the solution to the steady-state diffusion equation in the bulk of the domain. Therefore, Ω_ε may be decomposed into a set of $j = 1, \ldots, N$ "inner" regions, where $|\mathbf{r} - \mathbf{r}_j| = \mathcal{O}(\varepsilon)$, and an "outer" region, where $|\mathbf{r} - \mathbf{r}_j| \gg \mathcal{O}(\varepsilon)$ for all $j = 1, \ldots, N$. In the jth inner region, we

introduce the stretched local variable $\mathbf{s} = \varepsilon^{-1}(\mathbf{r} - \mathbf{r}_j)$ and set $V(\mathbf{s};\varepsilon) = U(\mathbf{r}_j + \varepsilon\mathbf{s};\varepsilon)$ so that to leading order (omitting far-field boundary conditions)

$$\begin{aligned} \nabla_{\mathbf{s}}^2 V = 0\,, \quad |\mathbf{s}| > 1, \\ V = U_j\,, \quad |\mathbf{s}| = 1. \end{aligned} \tag{3.11}$$

This has an exact solution of the form $V = U_j + B_j \log|\mathbf{s}|$ with the unknown amplitude B_j determined by matching inner and outer solutions. This leads to an infinite logarithmic expansion of B_j in terms of the small parameter [27, 25, 28, 24]

$$\nu = -\frac{1}{\log(\varepsilon)}. \tag{3.12}$$

Since the outer solution is $\mathcal{O}(1)$ as $\nu \to 0$ and V grows logarithmically at infinity, we write $B_j = \nu A_j(\nu)$, where the function $A_j(\nu)$ is to be found. The inner solution becomes

$$V = U_j + \nu A_j(\nu) \log|\mathbf{s}|. \tag{3.13}$$

In terms of the outer variable $|\mathbf{r} - \mathbf{r}_j|$, we then obtain the following far-field behavior of the inner solution:

$$V \sim U_j + A_j(\nu) + \nu A_j(\nu) \log|\mathbf{r} - \mathbf{r}_j|. \tag{3.14}$$

This far-field behavior must then match with the near-field behavior of the asymptotic expansion of the solution in the outer region away from the N traps. The corresponding outer problem is given by

$$\nabla^2 U = 0, \quad \mathbf{r} \in \Omega_0 \backslash \{\mathbf{r}_1, \ldots, \mathbf{r}_N\}, \tag{3.15}$$

with boundary conditions

$$\begin{aligned} U(x,\pi l) = U(x,-\pi l)\,, \quad \partial_y U(x,\pi l) = \partial_y U(x,-\pi l), \\ \partial_x U(0,y) = -\sigma, \quad \partial_x U(L,y) = 0, \end{aligned}$$

together with the asymptotic singularity conditions

$$U \sim U_j + A_j(\nu) + \nu A_j(\nu) \log|\mathbf{r} - \mathbf{r}_j| \quad \text{as } \mathbf{r} \to \mathbf{r}_j\,, \quad j = 1, \ldots, N. \tag{3.16}$$

Equations (3.15) and (3.16) can be reformulated in terms of an outer problem with homogeneous boundary conditions and a constant forcing term by decomposing

$$U(\mathbf{r}) = \mathcal{U}(\mathbf{r}) + u(\mathbf{r})\,, \quad u(x,y) \equiv \frac{\sigma}{2L}(x - L)^2. \tag{3.17}$$

Then (3.15) becomes

$$\nabla^2 \mathcal{U} = -\frac{\sigma}{L}\,, \quad \mathbf{r} \in \Omega_0 \backslash \{\mathbf{r}_1, \ldots, \mathbf{r}_N\}\,, \tag{3.18}$$

with boundary conditions

$$\begin{aligned} \mathcal{U}(x,\pi l) = \mathcal{U}(x,-\pi l)\,, \quad \partial_y \mathcal{U}(x,\pi l) = \partial_y \mathcal{U}(x,-\pi l), \\ \partial_x \mathcal{U}(0,y) = 0, \quad \partial_x \mathcal{U}(L,y) = 0\,, \end{aligned}$$

and the asymptotic singularity conditions

$$\mathcal{U} \sim -u(\mathbf{r}_j) + U_j + A_j(\nu) + \nu A_j(\nu) \log|\mathbf{r} - \mathbf{r}_j| \quad \text{as } \mathbf{r} \to \mathbf{r}_j\,, \quad j = 1, \dots, N. \tag{3.19}$$

In order to treat the logarithmic behavior of the outer solution at $\mathbf{r}_j$, we introduce the Neumann Green's function $G(\mathbf{r}; \mathbf{r}')$, defined as the unique solution to

$$\begin{aligned} \nabla^2 G &= \frac{1}{|\Omega_0|} - \delta(\mathbf{r} - \mathbf{r}')\,, \quad \mathbf{r} \in \Omega_0\,, \\ G(x, \pi l; \mathbf{r}') &= G(x, -\pi l; \mathbf{r}')\,, \quad \partial_y G(x, \pi l; \mathbf{r}') = \partial_y G(x, -\pi l; \mathbf{r}'), \\ \partial_x G(0, y; \mathbf{r}') &= 0\,, \quad \partial_x G(L, y; \mathbf{r}') = 0\,, \\ \int_{\Omega_0} G(\mathbf{r}; \mathbf{r}')\, d\mathbf{r} &= 0. \end{aligned} \tag{3.20}$$

Here $|\Omega_0| = 2\pi L l$ is the area of the rectangular domain Ω_0. This Green's function has a logarithmic singularity as $\mathbf{r} \to \mathbf{r}'$ so that we can decompose G as

$$G(\mathbf{r}; \mathbf{r}') = -\frac{1}{2\pi} \log|\mathbf{r} - \mathbf{r}'| + \mathcal{G}(\mathbf{r}; \mathbf{r}'), \tag{3.21}$$

where $\mathcal{G}$ is the regular part of G. We will calculate $\mathcal{G}$ explicitly in section 3.3. This property of G suggests that we replace (3.18) and (3.19) by the following single equation in Ω_0:

$$\nabla^2 \mathcal{U} = -\frac{\sigma}{L} + \sum_{j=1}^{N} 2\pi\nu A_j(\nu) \delta(\mathbf{r} - \mathbf{r}_j)\,, \quad \mathbf{r} \in \Omega_0. \tag{3.22}$$

Then, upon using the divergence theorem together with the homogeneous boundary conditions for $\mathcal{U}$, we obtain the solvability condition

$$\frac{\sigma}{L} |\Omega_0| = \sum_{j=1}^{N} 2\pi\nu A_j(\nu). \tag{3.23}$$

It readily follows that (3.22) has the solution

$$\mathcal{U}(\mathbf{r}) = -\sum_{j=1}^{N} 2\pi\nu A_j(\nu) G(\mathbf{r}; \mathbf{r}_j) + \chi, \tag{3.24}$$

where χ is a constant to be found. Since $\int_{\Omega_0} G\, d\mathbf{r} = 0$, it follows that χ can be interpreted as the spatial average of $\mathcal{U}$, defined by $\chi = |\Omega_0|^{-1} \int_{\Omega_0} \mathcal{U}\, d\mathbf{r}$. Then, as $\mathbf{r} \to \mathbf{r}_j$, the outer solution for $\mathcal{U}$ given in (3.24) has the near-field behavior

$$\mathcal{U} \sim -2\pi\nu A_j(\nu) \left[-\frac{1}{2\pi} \log|\mathbf{r} - \mathbf{r}_j| + \mathcal{G}(\mathbf{r}_j; \mathbf{r}_j) \right] - \sum_{i \neq j}^{N} 2\pi\nu A_i(\nu) G(\mathbf{r}_j; \mathbf{r}_i) + \chi \tag{3.25}$$

for each $j = 1, \dots, N$. Upon comparing the nonsingular terms in this expression and that of (3.19), we obtain the following system of equations:

$$(1 + 2\pi\nu \mathcal{G}_{jj}) A_j + \sum_{i \neq j}^{N} 2\pi\nu G_{ji} A_i = u_j - U_j + \chi\,, \quad j = 1\,, \dots, N\,, \tag{3.26}$$

where $u_j \equiv u(\mathbf{r}_j)$, $G_{ji} \equiv G(\mathbf{r}_j; \mathbf{r}_i)$, and $\mathcal{G}_{jj} \equiv \mathcal{G}(\mathbf{r}_j; \mathbf{r}_j)$.

3.2. Calculation of boundary concentrations U_j. Equations (3.13) and (3.24) are the inner and outer solutions of BVPII, respectively, where the $N+1$ coefficients χ and A_j for $j=1,\dots,N$ are determined from the N linear equations (3.26) together with the solvability condition (3.23). We can now generate the solution to the original problem BVPI by substituting the inner solution (3.13) into the mixed boundary conditions (3.7). This gives

$$2\pi\nu A_j(\nu) = \frac{\widehat{\omega}_j}{D}[U_j - \widehat{R}_j] \equiv V_j. \tag{3.27}$$

Substituting (3.27) into the solvability condition (3.23) shows that the latter is equivalent to the conservation equation (3.9). Furthermore, upon substituting (3.27) into (3.26) we obtain the system of linear equations

$$\left[(2\pi\nu)^{-1} + \mathcal{G}_{jj}\right]\frac{\widehat{\omega}_j}{D}[U_j - \widehat{R}_j] + \sum_{i\neq j}^{N} G_{ji}\frac{\widehat{\omega}_i}{D}[U_i - \widehat{R}_i] = u_j - U_j + \chi\,, \quad j=1,\dots,N. \tag{3.28}$$

This system, together with the conservation equation (3.9), gives $N+1$ equations for the $N+1$ unknowns χ and $U_j, j=1,\dots,N$. This system depends on the flux σ_0 of receptors from the soma, the number and the locations of the dendritic spines, and the aspect ratio of Ω_0. Upon solving this system for U_j and χ, the dendritic receptor concentration in the bulk of the dendritic membrane, obtained from (3.17), (3.24), and (3.27), is given by

$$U(\mathbf{r}) = u(\mathbf{r}) - \sum_{j=1}^{N}\frac{\widehat{\omega}_j}{D}[U_j - \widehat{R}_j]G(\mathbf{r};\mathbf{r}_j) + \chi. \tag{3.29}$$

This approximate solution for U is valid for distances larger than $\mathcal{O}(\varepsilon)$ away from the centers $\mathbf{r}_j$, for $j=1,\dots,N$, of the spines. Moreover, the distribution R_j of receptors within the spines is given in terms of U_j by (3.1).

There are two important remarks. First, we emphasize that the system (3.26) together with (3.23) contains all of the logarithmic correction terms in the asymptotic solution to BVPI. The error made in this approximation is transcendentally small of order $\mathcal{O}(\varepsilon)$, which is asymptotically smaller than any power of ν. A precise estimate of such transcendentally small terms for a related problem is given in Appendix A of [25]. Second, we remark that in [6] we have previously derived one-dimensional versions of (3.9), (3.28), and (3.29). In contrast to the two-dimensional case, the one-dimensional Neumann Green's function is nonsingular so that one can represent the spines as point sources/sinks on the dendrite, and singular perturbation theory is not needed.

It is convenient to introduce a matrix solution to (3.28). We first introduce the matrix $\mathbf{B}$ with elements

$$B_{jj} = 2\pi\left(\frac{D}{\widehat{\omega}_j} + \mathcal{G}_{jj}\right), \quad B_{ji} = 2\pi G_{ji}\,,\ \ j\neq i. \tag{3.30}$$

Then (3.28) can be written in the compact form

$$\sum_{i=1}^{N}(\delta_{i,j} + \nu B_{ji})V_i = 2\pi\nu[u_j - \widehat{R}_j + \chi]\,,$$

where V_i is defined in (3.27). Defining $\mathbf{M} = (\mathbf{I}+\nu\mathbf{B})^{-1}$, where $\mathbf{I}$ is the $N \times N$ identity matrix, we have

$$V_j = 2\pi\nu \sum_{i=1}^{N} M_{ji}(u_i - \widehat{R}_i + \chi). \tag{3.31}$$

The constant χ is then determined by substituting (3.31) into the solvability condition (3.9). This yields

$$\frac{\sigma_0}{D} = \sum_{j=1}^{N} V_j = 2\pi\nu \sum_{i=1}^{N}\sum_{j=1}^{N} M_{ji}(u_i - \widehat{R}_i + \chi).$$

Upon solving this equation for χ we get

$$\chi = \frac{\frac{\sigma_0}{2\pi\nu D} - \sum_{i=1}^{N}\sum_{j=1}^{N} M_{ji}(u_i - \widehat{R}_i)}{\sum_{i=1}^{N}\sum_{j=1}^{N} M_{ji}}. \tag{3.32}$$

Since $M_{ji} = \delta_{i,j} + \mathcal{O}(\nu)$, it follows that to leading order in ν

$$\chi = \frac{\sigma_0}{2\pi N D\nu} + \mathcal{O}(1), \quad U_j = \widehat{R}_j + \frac{\sigma_0}{N\widehat{\omega}_j} + \mathcal{O}(\nu). \tag{3.33}$$

The singular nature of the constant χ as $\nu \to 0$, and hence the solution $U(\mathbf{r})$, reflects the fact that for fixed somatic flux σ_0, the flux in the neighborhood of each spine boundary $\partial\Omega_j$ diverges as $\varepsilon \to 0$. This is necessary in order to maintain the solvability condition (3.9). Note, in particular, that $\widehat{\omega}_j[U_j - \widehat{R}_j]$ gives the number of receptors flowing across the boundary per unit time, and its size essentially remains fixed as ε decreases. Thus, in this limit, the flux through the boundary increases, resulting in a steeper concentration gradient in a neighborhood of the spine boundary. If the hopping rate $\widehat{\omega}_j$ decreases as ε decreases, then the boundary concentration U_j will also diverge in order to maintain (3.9).

3.3. Evaluation of Green's function. To evaluate the Green's function G satisfying (3.20), we begin by writing its Fourier series representation,

$$\begin{aligned} G(\mathbf{r};\mathbf{r}') = {} & \frac{2}{|\Omega_0|}\sum_{n=1}^{\infty} \frac{\cos\left(\frac{\pi n x}{L}\right)\cos\left(\frac{\pi n x'}{L}\right)}{\left(\frac{\pi n}{L}\right)^2} + \frac{2}{|\Omega_0|}\sum_{m=1}^{\infty} \frac{\cos\left(\frac{m(y-y')}{l}\right)}{\left(\frac{m}{l}\right)^2} \\ & + \frac{4}{|\Omega_0|}\sum_{m=1}^{\infty}\sum_{n=1}^{\infty} \frac{\cos\left(\frac{\pi n x}{L}\right)\cos\left(\frac{\pi n x'}{L}\right)\cos\left(\frac{m(y-y')}{l}\right)}{\left(\frac{\pi n}{L}\right)^2 + \left(\frac{m}{l}\right)^2}. \end{aligned} \tag{3.34}$$

Upon recalling the formula (cf. p. 46 of [12])

$$\sum_{k=1}^{\infty} \frac{\cos(k\theta)}{k^2+b^2} = \frac{\pi}{2b}\frac{\cosh(b(\pi - |\theta|))}{\sinh(\pi b)} - \frac{1}{2b^2}, \quad |\theta| \le 2\pi\,, \tag{3.35}$$

we can sum the third term of (3.34) over the index n to obtain

$$\frac{1}{2\pi}\sum_{m=1}^{\infty}\frac{\cos\left(\frac{m(y-y')}{l}\right)\left[\cosh\left(\frac{m(L-|x-x'|)}{l}\right)+\cosh\left(\frac{m(L-|x+x'|)}{l}\right)\right]}{m\sinh\left(\frac{Lm}{l}\right)} - \frac{2}{|\Omega_0|}\sum_{m=1}^{\infty}\frac{\cos\left(\frac{m(y-y')}{l}\right)}{\left(\frac{m}{l}\right)^2}. \tag{3.36}$$

Notice that the second sum of (3.36) cancels the second sum of (3.34). Then, using the angle addition formula for hyperbolic cosine and the relation $\cosh(x)-\sinh(x)=\mathrm{e}^{-x}$, we derive the following key identity for any constants a, b, and c:

$$\frac{\cosh(a-b)+\cosh(a-c)}{\sinh a}=\frac{1}{1-\mathrm{e}^{-2a}}\left[\mathrm{e}^{-b}+\mathrm{e}^{-c}+\mathrm{e}^{b-2a}+\mathrm{e}^{c-2a}\right]. \tag{3.37}$$

We use this identity to rewrite the first sum in (3.36) and then substitute the resulting expression into (3.34). This yields

$$G(\mathbf{r};\mathbf{r}')=\frac{H(x;x')}{2\pi l}+\sum_{m=1}^{\infty}\frac{\left(z_+^m+\overline{z_+}^m+z_-^m+\overline{z_-}^m+\zeta_+^m+\overline{\zeta_+}^m+\zeta_-^m+\overline{\zeta_-}^m\right)}{4\pi m(1-q^m)}, \tag{3.38}$$

where $q\equiv\mathrm{e}^{-2L/l}$. Here $z_\pm$ and $\zeta_\pm$ are defined by $z_\pm\equiv\mathrm{e}^{r_\pm/l}$ and $\zeta_\pm\equiv\mathrm{e}^{\rho_\pm/l}$, where

$$r_+\equiv-|x+x'|+i(y-y'),\quad r_-\equiv-|x-x'|+i(y-y'), \tag{3.39}$$

$$\rho_+\equiv|x+x'|-2L+i(y-y'),\quad \rho_-\equiv|x-x'|-2L+i(y-y'), \tag{3.40}$$

and $\bar{\cdot}$ denotes complex conjugate. Moreover, in (3.38), $H(x;x')$ is defined by

$$H(x;x')\equiv\frac{2}{L}\sum_{n=1}^{\infty}\frac{\cos\left(\frac{\pi nx}{L}\right)\cos\left(\frac{\pi nx'}{L}\right)}{\left(\frac{\pi n}{L}\right)^2} =\frac{L}{12}\left[h\left(\frac{x-x'}{L}\right)+h\left(\frac{x+x'}{L}\right)\right],\quad h(\theta)\equiv3\theta^2-6|\theta|+2. \tag{3.41}$$

The function $H(x;x')$ is the one-dimensional Green's function in the x-direction.

Since $q=\mathrm{e}^{-2L/l}<1$, we can write $(1-q^m)^{-1}=\sum_{n=0}^{\infty}(q^m)^n$ for all $m\geq1$. In this way, the sum in (3.38) can be written as

$$\sum_{m=1}^{\infty}\sum_{n=0}^{\infty}(q^n)^m\frac{\left(z_+^m+\overline{z_+}^m+z_-^m+\overline{z_-}^m+\zeta_+^m+\overline{\zeta_+}^m+\zeta_-^m+\overline{\zeta_-}^m\right)}{4\pi m}. \tag{3.42}$$

Notice that when $z_\pm\neq1$ and $\zeta_\pm\neq1$ (i.e., when $r_\pm\neq0$ and $\rho_\pm\neq0$) this double sum is absolutely convergent, so we can interchange the order of summation in (3.42) and then perform the sum over the index m, yielding

$$-\frac{1}{4\pi}\sum_{n=0}^{\infty}\left(\ln|1-q^nz_+|^2+\ln|1-q^nz_-|^2+\ln|1-q^n\zeta_+|^2+\ln|1-q^n\zeta_-|^2\right) =-\frac{1}{2\pi}\ln|1-z_+||1-z_-||1-\zeta_+||1-\zeta_-|+\mathcal{O}(q). \tag{3.43}$$

The only singularity exhibited by (3.43) in Ω_0 is at $(x,y)=(x',y')$, in which case $z_-=1$ and $\ln|1-z_-|$ diverges. Writing $\ln|1-z_-|=\ln|r_-|+\ln(|1-z_-|/|r_-|)$ and noting that $\ln|r_-|=\ln|\mathbf{r}-\mathbf{r}'|$ and $\ln(|1-z_-|/|r_-|)$ is regular, we find that

$$G(\mathbf{r};\mathbf{r}')=-\frac{1}{2\pi}\ln|\mathbf{r}-\mathbf{r}'|+\mathcal{G}(\mathbf{r};\mathbf{r}')\,, \tag{3.44}$$

where the regular part $\mathcal{G}$ of G is given explicitly by

$$\mathcal{G}(\mathbf{r};\mathbf{r}')=\frac{H(x;x')}{2\pi l}-\frac{1}{2\pi}\ln\frac{|1-z_+||1-z_-||1-\zeta_+||1-\zeta_-|}{|r_-|}+\mathcal{O}(q). \tag{3.45}$$

This expression for $\mathcal{G}$ is valid in the large aspect ratio limit $L/l\gg 1$ for which $q\ll 1$.

4. Numerics. In this section we compare the asymptotic solution U of (3.29) and (3.31) with the full solution obtained by numerically solving (3.3)–(3.6). In order to implement the boundary conditions (3.6) we use the steady-state solution of R_j given by (3.1), with the mean boundary concentration U_j identified with the corresponding solution of the singular perturbation problem as determined by (3.27) and (3.1). We then check that the resulting numerical solution is self-consistent; that is, the mean receptor concentration around the boundary is well approximated by the assumed value for U_j. The two-dimensional numerical solutions are generated by using the *Partial Differential Equation Toolbox* of MATLAB [30]. In Figure 4.1(A) we plot the steady-state concentration U given by (3.29) and (3.31) for a cable of length $L=100\mu$m and radius $l=(2\pi)^{-1}\mu$m having 99 identical spines spaced 1μm apart along a single horizontal line ($y=0\mu$m). In Figure 4.1(B) we plot the corresponding values of U_j, R_j, and S_j, with R_j,S_j given by (3.1) and (3.2). Here the diffusivity is $D=0.1\mu\text{m}^2\text{s}^{-1}$ [13, 2], the somatic flux is $\sigma_0=0.1\mu\text{m}^{-1}\ \text{s}^{-1}$, and all spines are identical with radius $\varepsilon\rho=0.1\mu$m, $A=1\mu$m, $\omega=10^{-3}\mu\text{m}^2\text{s}^{-1}$, $k=10^{-3}\mu\text{m}^2\text{s}^{-1}$, $\sigma^{rec}=10^{-3}\text{s}^{-1}$, $\sigma^{deg}=10^{-4}\text{s}^{-1}$, and $\delta=10^{-3}\text{s}^{-1}$. We set $\rho=2\pi l=1\mu$m so that $\varepsilon=0.1$. While U decays significantly along the length of the cable, it varies very little around the circumference of the cable. In Figure 4.1(C) we show the results of numerically solving the original steady-state system for U described in (3.3)–(3.6). This numerical solution agrees almost perfectly with the perturbation solution shown in Figure 4.1(A).

We consider the parameter regime of Figure 4.1 physiological in the sense that parameter values were chosen from experimental data [2, 11, 13, 23] in conjunction with previous modeling studies [5, 6]. Our results suggest that in this parameter regime the dendrite can be treated as a quasi-one-dimensional system in which variations in receptor concentration around the circumference of the cable can be neglected. This is further reinforced by the observation that the solutions of the two-dimensional model shown in Figure 4.1(A)–(C) are virtually indistinguishable from the corresponding solution of the reduced one-dimensional model previously introduced in [6] (see Figure 4.1(D)). In the one-dimensional model, (2.1)–(2.4) are replaced by the inhomogeneous diffusion equation

$$\frac{\partial U}{\partial t}=D\frac{\partial^2 U}{\partial x^2}-\sum_{j=1}^{N}\frac{\omega_j}{2\pi l}[U_j-R_j]\delta(x-x_j)\,, \tag{4.1}$$

with boundary conditions $U_j(t)=U(x_j,t)$ and

$$D\left.\frac{\partial U}{\partial x}\right|_{x=0}=-\frac{\sigma_0}{2\pi lD},\quad D\left.\frac{\partial U}{\partial x}\right|_{x=L}=0. \tag{4.2}$$

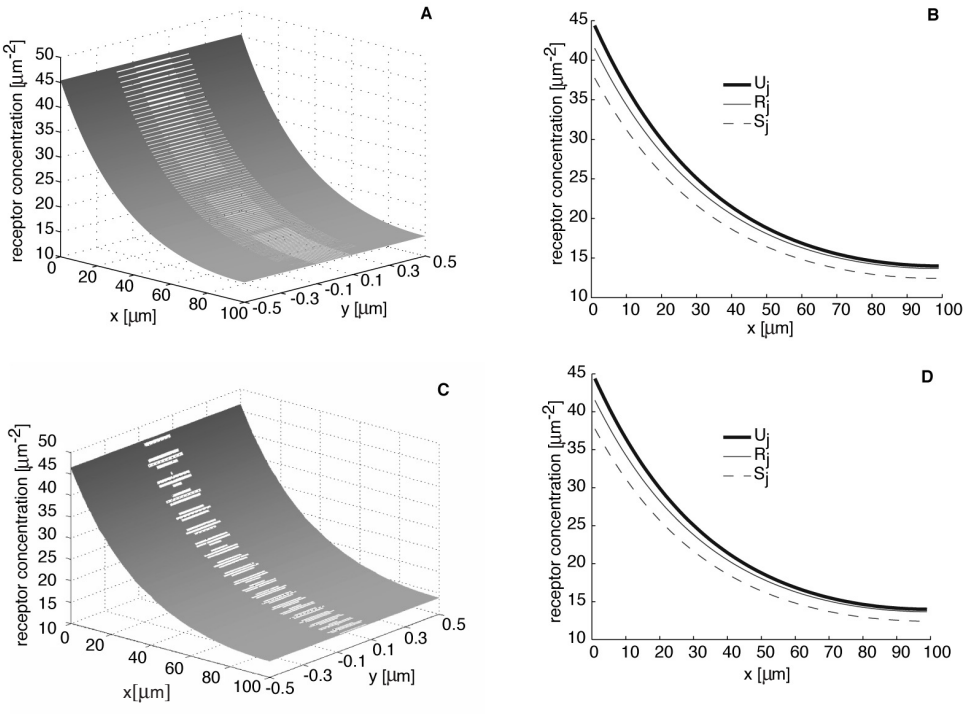

FIG. 4.1. *Plot of receptor concentration profiles along a dendritic cable with a uniform collinear distribution of dendritic spines. Cable and spine parameter values are given in the text.* (A) *Plot of bulk dendritic concentration* U *given by the outer solution* (3.29) *of the matched asymptotic expansion. Boundaries of spines are indicated by white lines. The dendritic cable is not drawn to scale.* (B) *Corresponding plots of* U_j, R_j, *and* S_j *obtained from* (3.27), (3.31), (3.1), *and* (3.2). *(Note that* S_j *is converted to a concentration by dividing through by the area* A_j *of a spine, which is taken to be* 1μm.*)* (C) *Numerical solution of* (3.3)–(3.6). (D) *Plots of* U_j, R_j, *and* S_j *obtained by solving the corresponding one-dimensional model* [6].

As in the two-dimensional model, R_j evolves according to (2.6) and (2.7). The steady-state solution of (4.1) can be obtained using the one-dimensional Green's function H such that

$$U(x) = \chi - \sum_{j=1}^{N} \frac{\widehat{\omega}_j [U_j - \widehat{R}_j]}{2\pi l D} H(x, x_j) + \frac{\sigma}{2\pi l D} H(x, 0)\,, \tag{4.3}$$

where the constant χ is determined from the self-consistency condition (3.9). The set of concentrations U_j can then be determined self-consistently by setting $x = x_i$ in (4.3) and solving the resulting matrix equation along analogous lines to (3.28) (cf. [6]). It is important to note that the excellent agreement between the two-dimensional and one-dimensional models is not a consequence of taking the spines to all lie along a one-dimensional line. This is illustrated in Figure 4.2 for a configuration of three staggered rows of 33 spines. The receptor concentrations are indistinguishable from the configuration consisting of a single row of 99 spines.

There is a simple heuristic argument to show why our original two-dimensional diffusion problem can be reduced to a corresponding one-dimensional problem, at

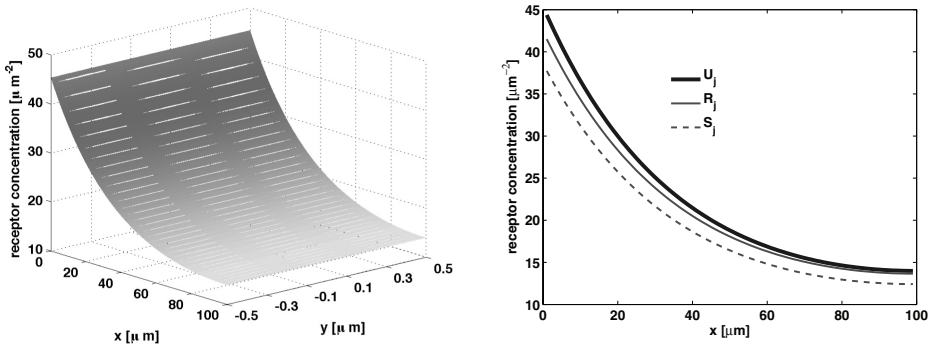

FIG. 4.2. *Plot of receptor concentration profiles along a dendritic cable with three staggered rows of spines. All other parameters are as in Figure* 4.1. *Left: Plot of bulk dendritic concentration* U *given by the outer solution* (3.29) *of the matched asymptotic expansion. Boundaries of spines are indicated by white lines. The dendritic cable is not drawn to scale. Right: Corresponding plots of* U_j, R_j, *and* S_j *obtained from* (3.27), (3.31), (3.1), *and* (3.2). *Concentration plots are indistinguishable from Figure* 4.1.

least in the parameter regime of Figure 4.1. Given a somatic flux $\sigma_0 = 0.1\mu\text{m}^{-1}\text{s}^{-1}$, a cable circumference of 1μm, and $N = 100$ spines, it follows that the mean number of receptors flowing through each spine boundary per second is 10^{-3}. Thus a rough estimate of the mean flux through each spine boundary of circumference $2\pi\varepsilon$ is $\bar{J} = 10^{-3}/(2\pi\varepsilon)\text{s}^{-1}\text{m}^{-1}$. Let ΔU represent the typical size of changes in receptor concentration needed to generate such a flux over a length scale Δx comparable to that of the dendritic circumference. Taking $\bar{J} \sim D\Delta U/\Delta x$ with $\Delta x = 2\pi l = 1\mu$m and $D = 0.1\mu\text{m}^2\text{s}^{-1}$ then gives $\Delta U \sim 10^{-2}l/\varepsilon \approx 1.6 \times 10^{-3}\mu\text{m}^{-2}$. Such a variation is negligible compared to the variation in receptor concentration along the length of the cable due to the source at the soma (see Figure 4.1), thus justifying a reduction to a one-dimensional model.

The above argument shows that the relatively small variation of receptor concentration around the circumference of the cable is a consequence of two factors: the large number of spines and the large aspect ratio ($l \ll L$) of the dendritic geometry; the length scales L, l put upper bounds on the maximum variation of the concentration in the x- and y-directions, respectively, for fixed σ_0. Thus we expect the two-dimensional nature of the spine's surface to become significant in the case of a few spines distributed on a short dendritic cable; such a situation could be relevant in the case of immature neurons. The solution for the receptor concentration will then be sensitive to the size of the spine radius ε. We illustrate this in Figure 4.3 in the case of a single spine centered at $(x, y) = (1, 0)$ on the surface of a dendrite of length $L = 2\mu$m. With this smaller value of L, the aspect ratio of the cable is now $L/l = 4\pi$. We also choose $\omega = k = 1\mu\text{m}^2\text{s}^{-1}$. In Figure 4.3(A)–(C) we show the singular perturbation solution for U when $\varepsilon = 0.01$, 0.1, and 0.4, respectively. In Figure 4.3(D)–(F) we show corresponding plots for the numerical solutions of U. It can be seen that the effect of the logarithmic singularity in the vicinity of the spine becomes prominent as ε decreases. Finally, in Figure 4.3(G) we plot the solution from the one-dimensional model. Although this model contains no information about the radius of the spine neck, and the aspect ratio of the system is now only moderately large, it still provides an approximate solution that agrees quite well with the full two-dimensional solutions.

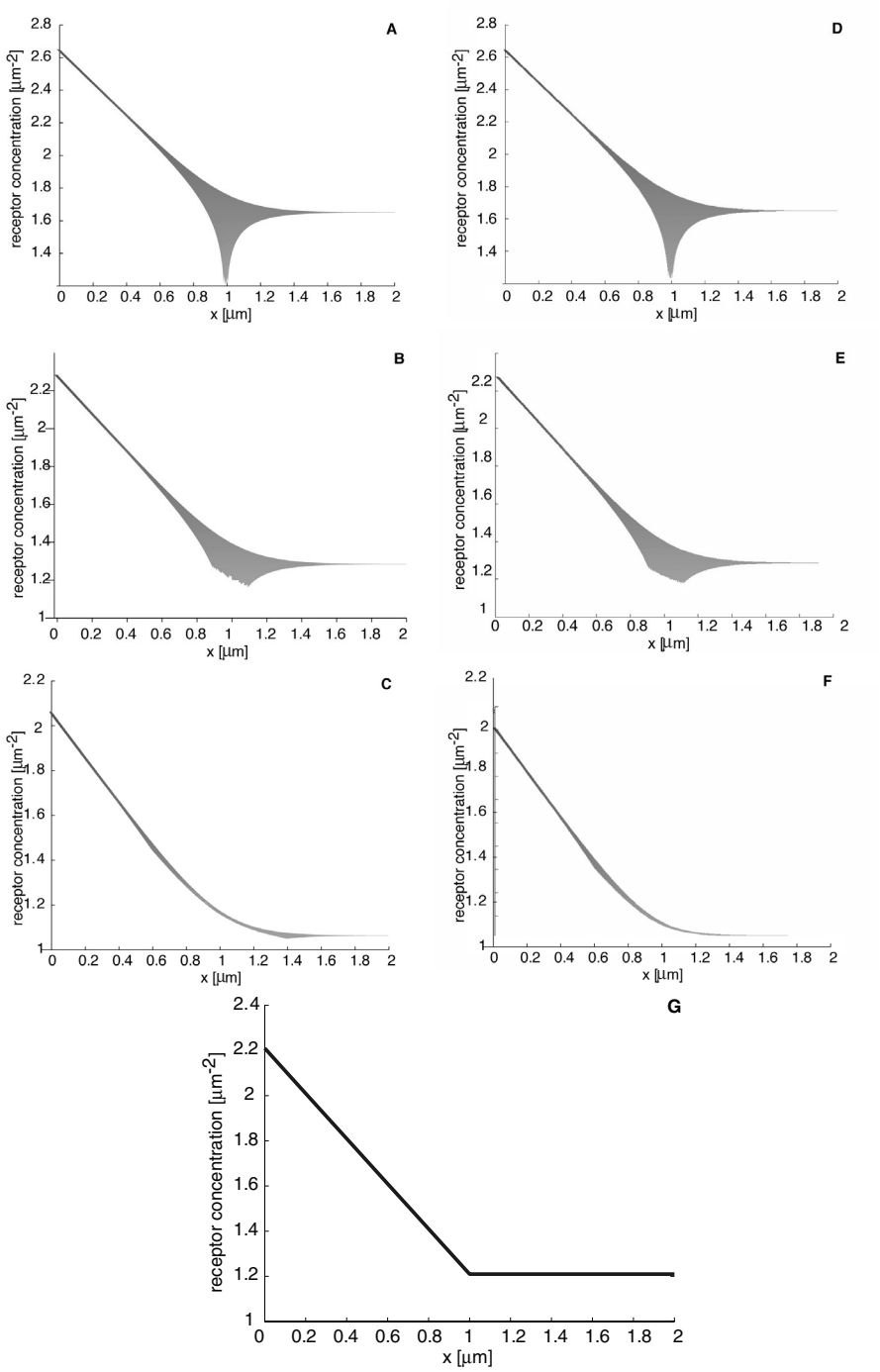

FIG. 4.3. *Effect of spine radius ε on the solution U for a single spine centered at $x = 1\mu$m, $y = 0$ on a short dendritic cable of length $L = 2\mu$m.* (A)–(C) *Plots of bulk dendritic receptor concentration U along the dendrite given by the outer solution* (3.29) *of the matched asymptotic expansion for parameter values as specified in the text and $\varepsilon = 0.01$, 0.1, and 0.4μm, respectively. The shaded region shows the range of values taken by the receptor concentration around the circumference of the cable as a function of distance x from the soma.* (D)–(F) *Corresponding plots of numerical solutions for U.* (G) *Plot of the one-dimensional solution* [6].

5. Mean first passage time (MFPT) for a single receptor. In this section we calculate the MFPT for a single tagged receptor to travel an axial distance X from the soma, $X < L$, assuming that the receptor does not undergo degradation. We then use this to determine an effective diffusivity, which takes into account the effects of trapping at spines. We proceed by reinterpreting the dendritic receptor concentration as a probability density and the diffusion equation (2.1) as a Fokker–Planck (FP) equation. The FP equation is defined on a spatial domain Ω_ε^X, where

$$\Omega_\varepsilon^X = \Omega_X \setminus \bigcup_{j=1}^{N_X} \Omega_j, \quad \Omega_j = \{\mathbf{r} : |\mathbf{r} - \mathbf{r}_j| \le \varepsilon\}.$$

Here $\Omega_X = \{(x,y); 0 < x < X, |y| < \pi l\}$ and N_X is the number of spines within the rectangular domain Ω_X. We impose an absorbing boundary condition at $x = X$ so that the receptor is immediately removed once it reaches this boundary; i.e., we are interested only in the time it takes for a receptor to first reach $x = X$ from the soma. Let $u(\mathbf{r}, t|\mathbf{r}_0, 0)$ denote the probability density that at time $t \ge 0$ the receptor is located at $\mathbf{r} \in \Omega_\varepsilon^X$, given that it started at the point $\mathbf{r}_0 = (0, y_0)$. The probability density u evolves according to the FP equation

$$\frac{\partial u}{\partial t} = D\nabla^2 u, \quad (\mathbf{r}, t) \in \Omega_\varepsilon^X \times \mathbf{R}_+ , \tag{5.1}$$

with periodic boundary conditions at the ends $y = \pm\pi l$,

$$u(x, \pi l, t|\mathbf{r}_0, 0) = u(x, -\pi l, t|\mathbf{r}_0, 0), \quad \partial_y u(x, \pi l, t|\mathbf{r}_0, 0) = \partial_y u(x, -\pi l, t|\mathbf{r}_0, 0) , \tag{5.2}$$

and with

$$\partial_x u(0, y, t|\mathbf{r}_0, 0) = 0 , \quad u(X, y, t|\mathbf{r}_0, 0) = 0. \tag{5.3}$$

At each interior boundary $\partial\Omega_j$ we impose the mixed boundary condition

$$\varepsilon \partial_n u(\mathbf{r}, t|\mathbf{r}_0, 0) = -\frac{\omega_j}{2D\pi}(u(\mathbf{r}, t|\mathbf{r}_0, 0) - r_j(t|\mathbf{r}_0, t)), \quad \mathbf{r} \in \partial\Omega_j , \quad j = 1, \dots , N_X. \tag{5.4}$$

Here $A_j r_j(t|\mathbf{r}_0, t)$ denotes the probability that the receptor is located within the jth spine at time t. Defining $s_j(t|\mathbf{r}_0, t)$ to be the corresponding probability that the receptor is located within the jth intracellular pool, we have

$$A_j \frac{dr_j}{dt} = \omega_j[u_j - r_j] - k_j r_j + \sigma_j^{rec} s_j , \tag{5.5}$$

$$\frac{ds_j}{dt} = -\sigma_j^{rec} s_j + k_j r_j. \tag{5.6}$$

Since we are assuming that the tagged receptor has not been degraded over the time interval of interest, we have set $\sigma_j^{deg} = 0$ for all j. We also assume no production of intracellular receptors so that $\delta_j = 0$. The initial conditions are $u(\mathbf{r}, 0|\mathbf{r}_0, 0) = \delta(\mathbf{r} - \mathbf{r}_0)$ and $r_j(0|\mathbf{r}_0, 0) = s_j(0|\mathbf{r}_0, 0) = 0$ for all j.

5.1. MFPT. Let $\tau(X|\mathbf{r}_0)$ denote the time it takes for a receptor starting at $\mathbf{r}_0 = (0, y_0)$ to first reach the boundary $x = X$. The function

$$F(X,t|\mathbf{r}_0) \equiv \int_{\Omega_\varepsilon^X} u(\mathbf{r},t|\mathbf{r}_0,0)\,d\mathbf{r} + \sum_{j=1}^{N_X} [A_j r_j(t|\mathbf{r}_0,0) + s_j(t|\mathbf{r}_0,0)] \tag{5.7}$$

is the probability that $t < \tau(X|\mathbf{r}_0)$; i.e., the probability that a receptor which was initially at the origin has not yet reached $x = X$ in a time t. Notice that $1 - F$ is the cumulative density function for τ, and hence

$$\frac{\partial(1-F)}{\partial t} = -\frac{\partial F}{\partial t} \tag{5.8}$$

is its probability density function. Thus the MFPT, denoted by T, is

$$T = -\int_0^\infty t\frac{\partial F}{\partial t}\,dt = \int_0^\infty F\,dt. \tag{5.9}$$

The last equality in (5.9) follows by integrating the first integral by parts and recalling that F, being an L^1 function in time, decays more rapidly to zero than t^{-1} as t becomes large. Therefore, integrating (5.7) over time gives us the following expression for $T(X|\mathbf{r}_0)$:

$$T(X|\mathbf{r}_0) = \lim_{z\to 0}\left(\int_{\Omega_\varepsilon^X} \widehat{u}(\mathbf{r},z|\mathbf{r}_0,0)d\mathbf{r} + \sum_{j=1}^{N_X}[A_j\widehat{r}_j(z|\mathbf{r}_0,0) + \widehat{s}_j(z|\mathbf{r}_0,0)]\right), \tag{5.10}$$

where $\widehat{\cdot}$ denotes the Laplace transform,

$$\widehat{f}(z) \equiv \int_0^\infty \mathrm{e}^{-zt} f(t)dt. \tag{5.11}$$

Upon Laplace transforming (5.1)–(5.6) and using the initial conditions, we can take the limit $z \to 0$ to obtain

$$\widehat{u}_j(\mathbf{r}_0) = \widehat{r}_j(0|\mathbf{r}_0,0) = \frac{\sigma_j^{rec}}{k_j}\widehat{s}_j(0|\mathbf{r}_0,0), \tag{5.12}$$

where

$$\widehat{u}_j(\mathbf{r}_0) = \frac{1}{2\pi\varepsilon}\int_{\partial\Omega_j} \widehat{u}(\mathbf{r};\mathbf{r}_0)\,d\mathbf{r}. \tag{5.13}$$

Here we have set $\widehat{u}(\mathbf{r};\mathbf{r}_0) = \lim_{z\to 0}\widehat{u}(\mathbf{r},z|\mathbf{r}_0,0)$. Hence, we obtain the boundary value problem

$$D\nabla^2\widehat{u}(\mathbf{r};\mathbf{r}_0) = -\delta(\mathbf{r}-\mathbf{r}_0), \quad \mathbf{r}\in\Omega_\varepsilon^X, \tag{5.14}$$

with

$$\widehat{u}(x,\pi l;\mathbf{r}_0) = \widehat{u}(x,-\pi l;\mathbf{r}_0), \quad \partial_y\widehat{u}(x,\pi l;\mathbf{r}_0) = \partial_y\widehat{u}(x,-\pi l;\mathbf{r}_0), \tag{5.15}$$

$$\partial_x\widehat{u}(0,y;\mathbf{r}_0) = 0, \quad \widehat{u}(X,y;\mathbf{r}_0) = 0, \tag{5.16}$$

and the mixed boundary condition

$$\varepsilon\partial_n\widehat{u}(\mathbf{r};\mathbf{r}_0) = -\beta_j\left(\widehat{u} - \frac{1}{2\pi\varepsilon}\int_{\partial\Omega_j}\widehat{u}\,d\mathbf{r}\right), \quad j=1,\dots,N_X\,, \tag{5.17}$$

where β_j is defined in terms of the hopping rate by $\beta_j \equiv \omega_j/(2D\pi)$.

As in section 3, we have a singularly perturbed boundary value problem, although in a weaker sense than the previous case. Carrying out a matched asymptotic expansion, the details of which are presented in the appendix, we find that there are no logarithmic singularities and the dependence on the spine size is $\mathcal{O}(\varepsilon^2)$. More specifically, the outer solution has the asymptotic expansion

$$\widehat{u} \sim \frac{G_X(\mathbf{r};\mathbf{r}_0)}{D} + 2\pi\varepsilon^2\sum_{j=1}^{N_X}\left(\frac{\beta_j-1}{\beta_j+1}\right)\mathbf{a}_j\cdot\nabla_j G_X(\mathbf{r};\mathbf{r}_j)\,, \tag{5.18}$$

where ∇_j denotes differentiation with respect to the source variable $\mathbf{r}_j$, and $\mathbf{a}_j$ is defined by

$$\mathbf{a}_j \equiv \frac{\nabla G_X(\mathbf{r}_j;\mathbf{r}_0)}{D}. \tag{5.19}$$

Here G_X is the Green's function on the rectangular domain Ω_X with periodic boundary conditions at the ends $y=\pm\pi l$, a reflecting boundary at $x=0$, and an absorbing boundary at $x=X$. Thus,

$$G_X(\mathbf{r};\mathbf{r}') = \frac{2}{|\Omega_X|}\sum_{m=-\infty}^{\infty}\sum_{n=0}^{\infty}\frac{\cos\left(\frac{\pi(2n+1)x}{2X}\right)\cos\left(\frac{\pi(2n+1)x'}{2X}\right)\mathrm{e}^{im(y-y')/l}}{\left(\frac{\pi(2n+1)}{2X}\right)^2+\left(\frac{m}{l}\right)^2}. \tag{5.20}$$

Since G_X has a logarithmic singularity, it follows that

$$\nabla_j G_X(\mathbf{r};\mathbf{r}_j) \sim -\frac{1}{2\pi}\frac{(\mathbf{r}-\mathbf{r}_j)}{|\mathbf{r}-\mathbf{r}_j|^2} + \nabla_j\mathcal{G}_X \quad \text{as} \quad \mathbf{r}\to\mathbf{r}_j\,, \tag{5.21}$$

where $\mathcal{G}_X$ is the regular part of G_X. The average concentration $\widehat{u}_j$ around the boundary of the jth spine is obtained from the corresponding inner solution given in the appendix; see (A.6) and (A.8). Thus

$$\widehat{u}_j = \frac{G_X(\mathbf{r}_j;\mathbf{r}_0)}{D} + \frac{\varepsilon}{2\pi}\sum_{k=1}^{N_X}\left(\frac{2}{\beta_j+1}\right)\int_0^{2\pi}\mathbf{a}_j\cdot\mathbf{e}_\rho\,d\theta\,, \tag{5.22}$$

where $\mathbf{e}_\rho$ is the unit normal to the circular boundary $\partial\Omega_j$. Since $\mathbf{a}_j$ is a constant vector, it follows that $\int\mathbf{a}_j\cdot\mathbf{e}_\rho d\theta = 0$, and so the $\mathcal{O}(\varepsilon)$ term vanishes. Finally, substituting (5.12), (5.18), and (5.22) into (5.10) shows that

$$T(X|\mathbf{r}_0) = \int_{\Omega_X}\frac{G_X(\mathbf{r};\mathbf{r}_0)}{D}d\mathbf{r} + \sum_{j=1}^{N_X}\eta_j\frac{G_X(\mathbf{r}_j;\mathbf{r}_0)}{D} + \varepsilon^2\mathcal{J} + \cdots\,, \tag{5.23}$$

where $\eta_j = A_j + k_j/\sigma_j^{rec}$ and

$$\mathcal{J} = -\pi\sum_{j=1}^{N_X}\frac{G_X(\mathbf{r}_j;\mathbf{r}_0)}{D} + 2\pi\sum_{j=1}^{N_X}\left(\frac{\beta_j-1}{\beta_j+1}\right)\mathbf{a}_j\cdot\nabla_j\int_{\Omega_X}G_X(\mathbf{r};\mathbf{r}_j)\,d\mathbf{r}. \tag{5.24}$$

In the following we will determine the zeroth-order expression for the MFPT by dropping the $\mathcal{O}(\varepsilon^2)$ terms.

5.2. Evaluation of Green's function. We wish to evaluate the Green's function G_X in (5.20). We begin by expressing the double sum as

$$G_X(\mathbf{r};\mathbf{r}') = \frac{2}{|\Omega_X|}\sum_{n=0}^{\infty}\frac{\cos\left(\frac{\pi(2n+1)x}{2X}\right)\cos\left(\frac{\pi(2n+1)x'}{2X}\right)}{\left(\frac{\pi(2n+1)}{2X}\right)^2} + \frac{4}{|\Omega_X|}\sum_{m=1}^{\infty}\sum_{n=0}^{\infty}\frac{\cos\left(\frac{\pi(2n+1)x}{2X}\right)\cos\left(\frac{\pi(2n+1)x'}{2X}\right)\cos\left(\frac{m(y-y')}{l}\right)}{\left(\frac{\pi(2n+1)}{2X}\right)^2+\left(\frac{m}{l}\right)^2}. \tag{5.25}$$

Upon using the identity (derived from p. 46 of [12])

$$\sum_{k=0}^{\infty}\frac{\cos((2k+1)\theta)}{(2k+1)^2+b^2} = \frac{\pi}{4b}\left[\frac{\cosh(b(\pi-|\theta|))}{\sinh(\pi b)} - \frac{\cosh(b|\theta|)}{\sinh(\pi b)}\right], \quad |\theta|\le\pi, \tag{5.26}$$

we can perform the sum over the index n in (5.25), yielding

$$\frac{1}{2\pi}\sum_{m=1}^{\infty}\frac{\cos\left(\frac{m(y-y')}{l}\right)\left[\cosh\left(\frac{m(2X-|x-x'|)}{l}\right)+\cosh\left(\frac{m(2X-|x+x'|)}{l}\right)\right]}{m\sinh\left(\frac{2Xm}{l}\right)} + \mathcal{E}\,, \tag{5.27}$$

where $\mathcal{E}$ is defined by

$$\mathcal{E} \equiv -\frac{1}{2\pi}\sum_{m=1}^{\infty}\frac{\cos\left(\frac{m(y-y')}{l}\right)\left[\cosh\left(\frac{m|x-x'|}{l}\right)+\cosh\left(\frac{m|x+x'|}{l}\right)\right]}{m\sinh\left(\frac{2Xm}{l}\right)}. \tag{5.28}$$

Following arguments similar to those used in section 3.3, together with the identity (3.37), the infinite sums in (5.27) and (5.28) can be represented as infinite sums of logarithmic terms. Our calculations are greatly simplified if X is not too small (e.g., by assuming that $X \gg l/2$). In this large aspect ratio limit, the identity (3.37) yields that

$$\frac{\cosh\left(\frac{m(2X-|x-x'|)}{l}\right)+\cosh\left(\frac{m(2X-|x+x'|)}{l}\right)}{\sinh\left(\frac{2Xm}{l}\right)} \approx \mathrm{e}^{-m|x-x'|/l}+\mathrm{e}^{-m|x+x'|/l}+\mathcal{O}(q_X)\,, \tag{5.29}$$

where $q_X \equiv \mathrm{e}^{-2X/l}$. In addition, $\mathcal{E} = \mathcal{O}(q_X) \ll 1$ and can be neglected to a first approximation. Using these approximations for the large aspect ratio limit, we readily derive that

$$G_X(\mathbf{r};\mathbf{r}') = \frac{H_X(x;x')}{2\pi l} - \frac{1}{2\pi}\ln|1-z_+||1-z_-| + \mathcal{O}(q_X)\,, \tag{5.30}$$

where (cf. p. 46 of [12])

$$H_X(x;x') = \frac{2}{X}\sum_{n=0}^{\infty}\frac{\cos\left(\frac{\pi(2n+1)x}{2X}\right)\cos\left(\frac{\pi(2n+1)x'}{2X}\right)}{\left(\frac{\pi(2n+1)}{2X}\right)^2} = \frac{X}{2}\left[h_X\left(\frac{x-x'}{X}\right)+h_X\left(\frac{x+x'}{X}\right)\right], \quad h_X(\theta) = 1-|\theta|\,, \tag{5.31}$$

is the one-dimensional Green's function in the x-direction, and $z_\pm$ is as defined in (3.39).

Suppose that $\mathbf{r}' = \mathbf{r}_0 = (0, y_0)$. Since $x_0 = 0$,

$$G_X(\mathbf{r};\mathbf{r}_0) = \frac{X-x}{2\pi l} - \frac{1}{2\pi}\ln\left|1 - \mathrm{e}^{-x/l}\mathrm{e}^{i(y-y_0)/l}\right|^2 + \mathcal{O}(q_X). \tag{5.32}$$

If x is sufficiently large (e.g., $x \geq l$), then the contribution of the logarithmic term in (5.32) is of order $q_x = \mathrm{e}^{-2x/l}$, and hence

$$G_X(\mathbf{r};\mathbf{r}_0) = \frac{X-x}{2\pi l} + \mathcal{O}(q_x). \tag{5.33}$$

Since $\mathcal{O}(q_x)$ is exponentially small, this term can be dropped from (5.33), yielding the one-dimensional Green's function used in [6]. The fact that these results are effectively one-dimensional is again due to the large aspect ratio of our system.

5.3. Effective diffusivity and anomalous diffusion. Let us now evaluate the zeroth-order contributions to the MFPT $T(X|\mathbf{r}_0)$ given in (5.23). First, it follows from integrating (5.20) that $\int_{\Omega_X} G_X(\mathbf{r};\mathbf{r}_0)d\mathbf{r} = X^2/2$. Following the discussion of the previous paragraph, we will assume that all x_j are sufficiently large so that $G_X(\mathbf{r}_j;\mathbf{r}_0)$ is well approximated by the one-dimensional Green's function $(X-x_j)/(2\pi l)$. Since we are dropping any explicit dependence on y, y_0, we simply denote the MFPT $T(X|\mathbf{r}_0)$ by T. In the case of a large number of identical spines uniformly distributed along the length of the cable with spacing d (i.e., $N_X = X/d \gg 1$ and $x_j = jd$ for all j), we can compute an effective diffusivity D_{eff}. That is, substituting our one-dimensional approximation for G_X into (5.23) and dropping $\mathcal{O}(\varepsilon^2)$ terms gives

$$\begin{aligned} T &\approx \frac{X^2}{2D} + \frac{\eta}{2\pi lD}\sum_{j=1}^{N_X}(X-jd) = \frac{X^2}{2D} + \frac{\eta}{2\pi lD}\left(N_X X - \frac{(N_X+1)N_X d}{2}\right) \\ &\approx \frac{X^2}{2D} + \frac{\eta}{2\pi lD}\left(N_X X - \frac{N_X^2 d}{2}\right) = \frac{X^2}{2D}\left(1 + \frac{\eta}{2\pi l d}\right) = \frac{X^2}{2D_{eff}}, \end{aligned} \tag{5.34}$$

where $\eta \equiv A + k/\sigma^{rec}$. In (5.34), the effective diffusivity D_{eff} is

$$D_{eff} = D\left(1 + \frac{\eta}{2\pi l d}\right)^{-1} = D\left(1 + \frac{A + k/\sigma^{rec}}{2\pi l d}\right)^{-1}. \tag{5.35}$$

As one would expect, the presence of traps reduces the effective diffusivity of a receptor. In particular, the diffusivity is reduced by increasing the ratio k/σ^{rec} of the rates of endocytosis and exocytosis, by increasing the surface area A of a spine, or by decreasing the spine spacing d. Interestingly, D_{eff} does not depend on the hopping rate ω, at least to lowest order in the spine size ε. At first sight this might seem counterintuitive, since a smaller ω implies that a receptor finds it more difficult to exit a spine. However, this is compensated by the fact that it is also more difficult for a receptor to enter a spine in the first place. (For a more detailed analysis of entry/exit times of receptors with respect to spines see [14, 15]).

In (5.34) the MFPT T is proportional to X^2. This relationship is the hallmark of Brownian diffusion, and here it is due to the fact that the spacing between spines is independent of the index j. Now suppose that the spacing varies with j according

to $x_j = d(\ln(j)+1)$. In this case $N_X = \mathrm{e}^{X/d-1}$, and hence N_X grows exponentially with X [19]. Therefore, upon summing the series and using Stirling's formula, we get

(5.36)
$$T \approx \frac{X^2}{2D} + \frac{\eta}{2\pi l D}\sum_{j=1}^{N_X}(X - d(\ln(j)+1)) = \frac{X^2}{2D} + \frac{\eta}{2\pi l D}\left(N_X X - d(\ln(N_X!) + N_X)\right)$$
$$\approx \frac{X^2}{2D} + \frac{\eta}{2\pi l D}\left(N_X X - dN_X \ln(N_X)\right) = \frac{X^2}{2D} + \frac{\eta d}{2\pi l D}\mathrm{e}^{X/d-1} = \frac{X^2}{2D_{eff}(X)},$$

where the effective diffusivity is

$$D_{eff}(X) = D\left(1 + \frac{A + k/\sigma^{rec}}{2\pi l d}\frac{\mathrm{e}^{X/d-1}}{\frac{(X/d)^2}{2}}\right)^{-1}. \tag{5.37}$$

The fact that the effective diffusivity is a function of X indicates anomalous diffusion, which is to say that the relationship $T \propto X^2$ does not hold. Moreover, because $\mathrm{e}^{X/d-1}$ grows faster than $(X/d)^2$, the anomalous behavior is subdiffusive.

Note that the above analysis reproduces results obtained previously for a simplified one-dimensional model [6]. However, our asymptotic analysis shows that there are $\mathcal{O}(\varepsilon^2)$ corrections to the one-dimensional results given by (5.24). In particular, these higher-order corrections introduce a weak dependence of the MFPT on the size of the spines and the hopping rates ω_j via the parameters β_j.

6. Discussion. In this paper we have used singular perturbation theory to determine the steady-state receptor concentration on the cylindrical surface of a dendritic cable in the presence of small dendritic spines, which act as partially absorbing traps. In the case of long, thin dendrites we have shown that the variation of the receptor concentration around the circumference of the cable is negligible so that the concentration profile along the cable can be determined using a simpler one-dimensional model [6]. We have also shown that the MFPT for a single tagged receptor to travel a certain distance along the cable is well approximated by considering a random walk along a one-dimensional cable. In both cases, our perturbation analysis provides details regarding corrections to the one-dimensional results that depend on the size ε of spines. Such corrections would be significant in the case of short dendrites with few spines, which may occur in immature neurons. An important extension of our work would be to consider a much more detailed model of receptor trafficking within each spine [10]. This would take into account the fact that the spine is not a homogeneous medium but contains a protein rich subregion known as the postsynaptic density where receptors can bind and unbind to various scaffolding proteins [4]. Interestingly, the coupling between the spine and the dendritic cable would not be affected by such details so that our solutions for the dendritic receptor concentration within the cable would carry over to more complex models.

The analysis presented in this paper provides a general mathematical framework for taking into account the effects of the size of spines on the surface diffusion of receptors (and other proteins) within the cell membrane. In the particular case of spiny dendrites it allows us to establish rigorously the validity of a one-dimensional reduction. This is important from a biological modeling perspective since the reduced model provides a relatively simple system in which to explore the role of diffusion in protein receptor trafficking along a dendrite. For example, one important biological

issue is whether or not diffusion is sufficient as a mechanism for delivering protein receptors to distal parts of the dendrite [1]. If one ignores the effects of trapping in spines, then an estimate for the mean time a receptor takes to travel a distance X from the soma via surface diffusion along a uniform cable is $T = X^2/2D$. Even for a relatively large diffusivity $D = 0.45\mu\text{m}^2\text{s}^{-1}$, the mean time to reach a proximal synapse at 100μm from the soma is approximately 3 hrs., whereas the time to reach a distal synapse at 1mm from the soma is around 300 hrs. The latter is much longer than the average lifetime of a receptor, which is around 1 day. The one-dimensional formulae for the MFPT in the presence of traps (see section 5) establishes that trapping within spines increases the delivery time of receptors to synapses even further due to an effective reduction in the diffusivity. Indeed, if the density of spines grows sufficiently fast towards distal ends of the dendrite, then this increase in the MFPT could be significant due to the emergence of anomalous subdiffusive behavior. Interestingly, there is experimental evidence for an enhanced spine density at distal locations [18].

Finally, it would be interesting to consider protein receptor trafficking across a population of synapses with other geometric configurations. In this study we focused on synapses located within dendritic spines that are distributed along a dendritic cable, since most excitatory neurons in the central nervous system have such structures. However, there are some classes of neurons that have synapses located directly on the cell body or soma. One striking example is the chick ciliary ganglion, which supplies motor input to the iris of the eye; the ganglion has nicotinic receptors that are distributed across the surface of the cell body within somatic spines [3]. Thus the basic mathematical approach presented here could be extended to other biologically relevant examples of surface diffusion in the presence of partially absorbing traps, including diffusion on the surface of a spherical cell body, where a reduction to a one-dimensional problem would not be possible.

Appendix. In this appendix we present the singular perturbation analysis used to obtain the outer solution (5.18). First, let $\widehat{u}_0$ be the solution to the boundary value problem without traps given by (5.14), (5.15), and (5.16). Then

$$\widehat{u}_0(\mathbf{r}) = \frac{G_X(\mathbf{r};\mathbf{r}_0)}{D}\,, \tag{A.1}$$

where G_X is the Green's function of (5.20). For the problem with traps, we write the outer expansion as

$$\widehat{u} = \frac{G_X(\mathbf{r};\mathbf{r}_0)}{D} + \sigma(\varepsilon)\widehat{u}_1 + \cdots\,, \tag{A.2}$$

where $\sigma(\varepsilon)$ is to be found. In order to determine the inner solution near the jth hole, we introduce the scaled coordinates $\mathbf{s} = \varepsilon^{-1}(\mathbf{r} - \mathbf{r}_j)$ and set $V(\mathbf{s}) = \widehat{u}(\mathbf{r}_j + \varepsilon\mathbf{s})$. Then V satisfies (omitting the far-field condition)

$$\nabla_{\mathbf{s}}^2 V = 0\,, \quad s \equiv |\mathbf{s}| \geq 1\,, \tag{A.3}$$

$$\partial_s V = \beta_j \left(V - \frac{1}{2\pi}\int_0^{2\pi} V\, d\theta \right) \quad \text{on} \quad s \equiv |\mathbf{s}| = 1. \tag{A.4}$$

Notice that any constant V_0 satisfies this problem. We therefore write $V = V_0 + \mu(\varepsilon)V_1 + \cdots$. The inner and outer solutions must satisfy the matching condition

$$\frac{1}{D}\left[G_X(\mathbf{r}_j;\mathbf{r}_0) + \nabla G_X(\mathbf{r}_j;\mathbf{r}_0)\cdot(\mathbf{r}_j - \mathbf{r}) + \cdots\right] + \sigma(\varepsilon)\widehat{u}_1 \sim V_0 + \mu(\varepsilon)V_1 + \cdots\,. \tag{A.5}$$

This implies that $\mu(\varepsilon) = \varepsilon$ and that the constant V_0 is given by

$$V_0 = \frac{G_X(\mathbf{r}_j;\mathbf{r}_0)}{D}. \tag{A.6}$$

In addition, V_1 is the solution to the inner problem (A.3) and (A.4) with the far-field behavior

$$V_1 \sim \mathbf{a}_j \cdot \mathbf{s}\,, \qquad \mathbf{a}_j \equiv \frac{\nabla G_X(\mathbf{r}_j;\mathbf{r}_0)}{D}. \tag{A.7}$$

A simple separation of variables calculation gives the exact solution

$$V_1 = \mathbf{a}_j \cdot \mathbf{s} - \left(\frac{\beta_j - 1}{\beta_j + 1}\right) \mathbf{a}_j \cdot \frac{\mathbf{s}}{|\mathbf{s}|^2}. \tag{A.8}$$

Substituting this into the matching condition (A.5) gives $\sigma(\varepsilon) = \varepsilon^2$ and that $\widehat{u}_1$ satisfies the asymptotic singularity conditions

$$\widehat{u}_1 \sim -\left(\frac{\beta_j - 1}{\beta_j + 1}\right) \mathbf{a}_j \cdot \frac{(\mathbf{r} - \mathbf{r}_j)}{|\mathbf{r} - \mathbf{r}_j|^2} \quad \text{as} \quad \mathbf{r} \to \mathbf{r}_j. \tag{A.9}$$

The function $\widehat{u}_1$ is to satisfy Laplace's equation, the boundary conditions (5.15) and (5.16), and the singularity conditions (A.9) for $j = 1, \ldots, N$.

Since the two-dimensional Green's function G_X has the logarithmic singularity $\frac{1}{2\pi} \log|\mathbf{r} - \mathbf{r}_j|$ for $\mathbf{r} \to \mathbf{r}_j$, it follows that $\nabla G_X(\mathbf{r};\mathbf{r}_j)$ has the dipole singularity

$$\frac{1}{2\pi} \frac{(\mathbf{r} - \mathbf{r}_j)}{|\mathbf{r} - \mathbf{r}_j|^2} \quad \text{as} \quad \mathbf{r} \to \mathbf{r}_j. \tag{A.10}$$

Unfortunately, $\nabla G_X(\mathbf{r};\mathbf{r}_j)$ does not satisfy the boundary conditions (5.15) and (5.16), so it cannot be used to construct an outer solution with the correct near-field behavior. On the other hand, we can construct a solution using $\nabla_j G_X(\mathbf{r};\mathbf{r}_j)$, where ∇_j is the gradient operator with respect to the singular point $\mathbf{r}_j$. That is, $-\nabla_j G_X(\mathbf{r};\mathbf{r}_j)$ has the same singular behavior as $\nabla G_X(\mathbf{r};\mathbf{r}_j)$ and also satisfies the boundary conditions (5.15) and (5.16). The latter follows from the observation that the boundary conditions for G_X do not involve $\mathbf{r}_j$ so that the boundary and Laplace operators commute with ∇_j. Finally, using linearity and superposition over the N_X holes, we readily obtain that the outer approximation is given explicitly by

$$\widehat{u} \sim \frac{G_X(\mathbf{r};\mathbf{r}_0)}{D} + 2\pi\varepsilon^2 \sum_{j=1}^{N_X} \left(\frac{\beta_j - 1}{\beta_j + 1}\right) \mathbf{a}_j \cdot \nabla_j G_X(\mathbf{r};\mathbf{r}_j). \tag{A.11}$$

REFERENCES

[1] H. Adesnik, R. A. Nicoll, and P. M. England, *Photoinactivation of native AMPA receptors reveals their real-time trafficking*, Neuron, 48 (2005), pp. 977–985.

[2] M. C. Ashby, S. R. Maier, A. Nishimune, and J. M. Henley, *Lateral diffusion drives constitutive exchange of AMPA receptors at dendritic spines and is regulated by spine morphology*, J. Neurosci., 26 (2006), pp. 7046–7055.

[3] D. K. Berg and W. G. Conroy, *Nicotinic α7 receptors: Synaptic options and downstream signaling in neurons*, J. Neurobiol., 53 (2002), pp. 512–523.

[4] D. S. Bredt and R. A, Nicoll, *AMPA receptor trafficking at excitatory synapses*, Neuron, 40 (2003), pp. 361–379.

[5] P. C. Bressloff, *Stochastic model of protein receptor trafficking prior to synaptogenesis*, Phys. Rev. E (3), 74 (2006), 031910.
[6] P. C. Bressloff and B. A. Earnshaw, *Diffusion–trapping model of receptor trafficking in dendrites*, Phys. Rev. E (3), 75 (2007), 041915.
[7] L. Chen, T. Tracy, and C. I. Nam, *Dynamics of postsynaptic glutamate receptor targeting*, Curr. Opin. Neurobiol., 17 (2007), pp. 53–58.
[8] D. Choquet and A. Triller, *The role of receptor diffusion in the organization of the postsynaptic membrane*, Nat. Rev. Neurosci., 4 (2003), pp. 251–265.
[9] G. L. Collingridge, J. T. R. Isaac, and Y. T. Wang, *Receptor trafficking and synaptic plasticity*, Nat. Rev. Neurosci., 5 (2004), pp. 952–962.
[10] B. A. Earnshaw and P. C. Bressloff, *A biophysical model of AMPA receptor trafficking and its regulation during LTP/LTD*, J. Neurosci., 26 (2006), pp. 12362–12373.
[11] M. D. Ehlers, *Reinsertion or degradation of AMPA receptors determined by activity-dependent endocytic sorting*, Neuron, 28 (2000), pp. 511–525.
[12] I. M. Gradshteyn and I. M. Ryzhik, *Table of Integrals, Series, and Products*, Academic Press, New York, 1980.
[13] L. Groc, M. Heine, L. Cognet, K. Brickley, F. A. Stephenson, B. Lounis, and D. Choquet, *Differential activity-dependent regulation of the lateral mobilities of AMPA and NMDA receptors*, Nat. Neurosci., 7 (2004), pp. 695–696.
[14] D. Holcman and Z. Schuss, *Escape through a small opening: Receptor trafficking in a synaptic membrane*, J. Statist. Phys., 117 (2004), pp. 975–1014.
[15] D. Holcman and A. Triller, *Modeling synaptic dynamics driven by receptor lateral diffusion*, Biophys. J., 91 (2006), pp. 2405–2415.
[16] M. J. Kennedy and M. D. Ehlers, *Organelles and trafficking machinery for postsynaptic plasticity*, Ann. Rev. Neurosci. 29 (2006), pp. 325–362.
[17] C.-H. Kim and J. E. Lisman, *A labile component of AMPA receptor-mediated synaptic transmission is dependent on microtubule motors, actin, and N-ethylmaleimide-sensitive factor*, J. Neurosci., 21 (2001), pp. 4188–4194.
[18] S. Konur, D. Rabinowitz, V. L. Fenstermaker, and R.Yuste, *Regulation of spine sizes and densities in pyramidal neurons*, J. Neurobiol., 56 (2003), pp. 95–112.
[19] M. Marin-Padilla, *Number and distribution of the apical dendritic spines of the layer V pyramidal cells in man*, J. Comp. Neurol., 131 (1967), pp. 475–489.
[20] M. Setou, D. H. Seog, Y. Tanaka, Y. Kanai, Y. Takei, and N. Hirokawa, *Glutamate-receptor-interacting protein GRIP*1 *directly steers kinesin to dendrites*, Nature, 417 (2002), pp. 83–87.
[21] M. Sheng and M. J. Kim, *Postsynaptic signaling and plasticity mechanisms*, Science, 298 (2002), pp. 776–780.
[22] I. Song and R. L. Huganir, *Regulation of AMPA receptors during synaptic plasticity*, Trends Neurosci., 25 (2002), pp. 578–588.
[23] K. E. Sorra and K. M. Harris, *Overview on the structure, composition, function, development, and plasticity of hippocampal dendritic spines*, Hippocampus, 10 (2000), pp. 501–511.
[24] R. Straube, M. J. Ward, and M. Falcke, *Reaction rate of small diffusing molecules on a cylindrical membrane*, J. Stat. Phys., 129 (2007), pp. 377–405.
[25] M. Titcombe and M. J. Ward, *Summing logarithmic expansions for elliptic equations in multiply-connected domains with small holes*, Canad. Appl. Math. Quart., 7 (1999), pp. 313–343.
[26] A. Triller and D. Choquet, *Surface trafficking of receptors between synaptic and extrasynaptic membranes*, Trends Neurosci., 28 (2005), pp. 133–139.
[27] M. J. Ward, W. D. Henshaw, and J. B. Keller, *Summing logarithmic expansions for singularly perturbed eigenvalue problems*, SIAM J. Appl. Math., 53 (1993), pp. 799–828.
[28] M. J. Ward, *Diffusion and bifurcation problems in singularly perturbed domains*, Natur. Resource Modeling, 13 (2000), pp. 271–302.
[29] P. Washbourne, X.-B. Liu, E. G. Jones, and A. K. McAllister, *Cycling of NMDA receptors during trafficking in neurons before synapse formation*, J. Neurosci., 24 (2004), pp. 8253–8264.
[30] MATLAB, *Partial Differential Equation Toolbox, User's Guide*, The MathWorks, Inc., Natick, MA, 1996.